Production and detection of ultracold Cs_2 molecules via four-photon adiabatic passage*

Li Jian(李 健), Liu Yong(刘 勇), and Cong Shu-Lin(丛书林)†

School of Physics and Optoelectronic Technology, Dalian University of Technology, Dalian 116024, *China*

(Received 30 March 2013; revised manuscript received 7 June 2013; published 2 December 2013)

We study theoretically how to produce and detect the ultracold ground-state Cs_2 molecule from Feshbach state. Numerical calculations are performed by solving the quantum Liouville equation based on multilevel Bloch model. The producing efficiency reaches 55% and the detecting efficiency is 31%. The producing and detecting efficiencies are closely related to the Rabi frequencies of laser pulses. The decay of relevant electronic and vibrational states obviously reduces the producing and detecting efficiencies.

Keywords: ultracold Cs_2 molecules, Liouville equation, density matrix, chainwise stimulated Raman adiabatic passage (STIRAP)

PACS: 03.75.Nt, 42.65.Dr, 32.80.Qk **DOI:** 10.1088/1674-1056/23/1/010308

1. Introduction

In recent years, the preparation and quantum control of cold ($T > 1$ mK) and ultracold ($T < 1$ mK) molecules have captured much attention of researchers and been one of the most active research subjects in the atomic and molecular physics.[1–6] Ultracold molecules have been applied in many fields such as testing fundamental physical constants,[7] precision spectroscopy,[8] and quantum-information processing.[9] Particularly, highly dense samples of molecules in the ground rovibrational state ($v = 0$, $J = 0$) are required in many applications. Magnetoassociation (MA) and photoassociation (PA) are two efficient ways to prepare ultracold molecules. In a PA process, weakly bound molecules are first created from ultracold atoms and then brought down to the ground electronic state by the spontaneous or stimulated emission.[10–12]

Aikawa *et al*. studied the direct conversion of laser-cooled ^{41}K and ^{87}Rb atoms into ultracold ^{41}K^{87}Rb molecules in the rovibrational ground state via photoassociation.[13] They proposed a detection method, spontaneous-decay-induced double resonance (SPIDR), to identify the two-photon resonance precisely. Jia and co-workers investigated the precision PA spectroscopy of ultracold cesium molecules experimentally.[14] They developed a technique for sensitively determining the laser-induced frequency shifts of the molecular vibrational and rotational levels.[15,16] Feshbach resonance plays an important role in the creation of ultracold molecules.[17–19] By using Feshbach resonance, the molecules are formed in high vibrational states near the dissociation limit, and then a fast decay resulting from the vibrational relaxation and the inelastic collision between the molecules and atoms may occur. In order to prepare stable ultracold molecules, the molecules created through Fescbach resonance must be rapidly transferred to the ground electronic state. The stimulated Raman adiabatic passage (STIRAP) is an effective way to create ground-state molecules.[20,21] The STIRAP is also a possible route towards minimizing losses and decoherence from spontaneous emission in photoassociation.[22,23] Recently, Winkler *et al*. demonstrated that coherent two-photon transfer through an STIRAP can be efficiently implemented in the quantum gases of weakly bound Feshbach molecules.[24] In their work, the prepared molecules, Rb_2, were still weakly bound with much less binding energy than the energy level of the ground ro-vibrational state. Danzl *et al*. prepared an ultracold and dense sample of molecules in a single hyperfine level of the ground ro-vibrational state via the Feshach resonance and four-photon STIRAP process.[25,26] In order to detect the deeply bound molecules, an additional laser pulse was employed to excite the molecules to a high vibrational state. The molecules with high vibrational states can be dissociated into atoms via the Feshbach ramping. The production efficiency can be obtained by detecting the number of dissociated atoms.[24,26]

In this work, we investigate how to produce and detect ultracold molecules. A passage from the initial state to the final state is opened while all intermediate states are virtually unoccupied. An effective five-level model is employed and the Liouville equation is numerically solved in our calculations.

2. Theoretical method

The theoretical scheme used in our calculation is depicted in Fig. 1, where $|g_1\rangle$ denotes the initial ground electronic state regarded as the Feshbach state, $|g_3\rangle$ and $|g_2\rangle$ denote the lowest

*Project supported by the National Natural Science Foundation of China (Grant Nos. 10974024 and 11274056).

†Corresponding author. E-mail: shlcong@dlut.edu.cn

© 2014 Chinese Physical Society and IOP Publishing Ltd

and higher vibrational states of ground electronic state, respectively, and $|e_1\rangle$ and $|e_2\rangle$ are two vibrational states of the excited electronic state. Four pulses are used to couple these states via a four-photon STIRAP. The weakly bound molecules in the $|g_1\rangle$ state are transferred to the $|g_3\rangle$ state through the intermediate states $|e_1\rangle$ and $|e_2\rangle$ (black line). In order to determine the population of the $|g_3\rangle$ state, after a delay time τ_d, a sequence of detection pulses is used to transfer the population back to the $|g_1\rangle$ state (red dotted line). The electric fields of the laser pulses causing the transitions $|g_2\rangle \leftarrow |e_1\rangle$ and $|e_2\rangle \leftarrow |g_2\rangle$ are given by

$$\varepsilon_i(t) = E_i \cos(\omega_i t), \quad (i = 2,3), \tag{1}$$

where E_i and ω_i are the field amplitude and carrier frequency, respectively. The electric fields of the lasers leading to the transitions $|e_1\rangle \leftarrow |g_1\rangle$ and $|g_3\rangle \leftarrow |e_2\rangle$ are given by the Gaussian pulses

$$\varepsilon_k(t) = E_k f_k(t) \cos[\omega_k(t-\tau_k)], \quad (k = 1,4), \tag{2}$$

where τ_k are the center time of the k-th pulse, and $f_k(t)$ is the normalized pulse envelope of the k-th pulse in the form of

$$f_k(t) = \exp\left[-4\ln 2\frac{(t-\tau_k)^2}{T_k^2}\right],$$

where T_k is the full width at half maximum (FWHM). Here, we take the four pulses to be real positive since their phase factors can be taken in a trivial global gauge transformation of the field operators. Within the rotation wave approximation (RWA) and under condition of two-photon resonance, the Hamiltonian of system can be expressed as[23,27]

$$\hat{H} = \frac{\hbar}{2}\begin{pmatrix} 0 & -\Omega_1 & 0 & 0 & 0 \\ -\Omega_1 & 2\Delta_1 & -\Omega_2 & 0 & 0 \\ 0 & -\Omega_2 & 0 & -\Omega_3 & 0 \\ 0 & 0 & -\Omega_3 & 2\Delta_2 & -\Omega_4 \\ 0 & 0 & 0 & -\Omega_4 & 0 \end{pmatrix}, \tag{3}$$

where Δ_1 and Δ_2 are the one-photon detunings, $\Omega_i = \mu_i E_i(t)/\hbar$ $(i = 2,3)$ and $\Omega_k = \mu_k E_k(t) f_k(t)/\hbar$ $(k = 1,4)$ are Rabi frequencies which couple five vibrational states in order, and μ_i and μ_k are the electric dipole moments. The Hamiltonian (3) has a dark state which is a specific superposition of states[27]

$$|\Psi^0\rangle = \frac{\Omega_2\Omega_4|g_1\rangle - \Omega_4\Omega_1|g_2\rangle + \Omega_1\Omega_3|g_3\rangle}{\sqrt{\Omega_4^2\Omega_1^2 + \Omega_1^2\Omega_3^2 + \Omega_2^2\Omega_4^2}}. \tag{4}$$

In a chainwise STIRAP, the laser fields are applied to create the dark state initially associated with the $|g_1\rangle$ state and finally with the $|g_3\rangle$ state. The system can stay in the dark state during evolution by changing the Rabi frequencies of the laser fields. The intermediate states $|e_1\rangle$ and $|e_2\rangle$ have no contribution to the dark state because they are not populated in the STIRAP. The density matrix of the system is obtained by solving the Liouville equation

$$i\hbar\frac{d\hat{\rho}}{dt} = [\hat{H}, \hat{\rho}] - \hat{\Gamma}\hat{\rho}, \tag{5}$$

where $\hat{\Gamma}$ is the decay operator. We assume that only the $|g_1\rangle$ state is initially populated, and the initial condition of the system can be written as $\rho_{g_1,g_1}(t=0) = 1$ and $\rho_{nm}(t=0) = 0$ $(n, m \neq g_1)$. Equation (5) combined with the Hamiltonian (3) can be solved numerically by using standard fourth-order Runge–Kutte method.

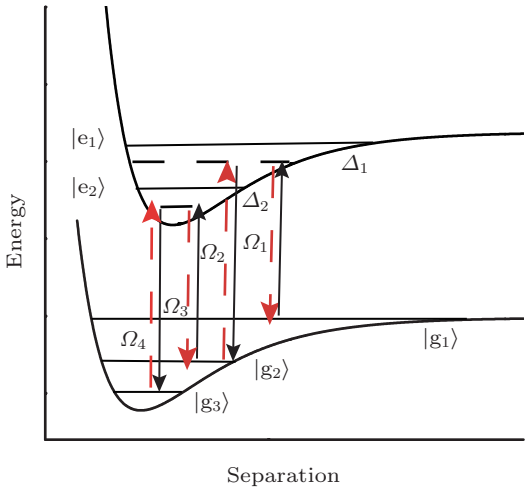


Fig. 1. (color online) Scheme of producing and detecting ultracold molecules through multistate chainwise STIRAP.

3. Results and discussion

We take the conversion of Cs atoms for example to study the formation of ultracold Cs_2 molecules. A sequence of laser pulses is used to produce and detect the ground-state molecules. Figure 2(a) shows the Rabi frequencies of four coherent pulses used in the calculation. The lifetimes of the excited states $|e_1\rangle$ and $|e_2\rangle$ are approximately 15 ns, which are obtained from the spontaneous emission. The decay rates of $|e_1\rangle$ and $|e_2\rangle$ are taken as $\Gamma_2 = \Gamma_4 = 6.5 \times 10^7$ Hz. The decays of $|g_2\rangle$ and $|g_3\rangle$, resulting from the atom-molecule and molecule-molecule collision, are roughly $\Gamma_3 = 1.0 \times 10^4$ Hz and $\Gamma_5 = 350$ Hz, respectively.[24] The decay rate Γ_1 is considered as a variable since its accurate value has not been found. Figure 2(b) shows the populations of the $|g_1\rangle$ and $|g_3\rangle$ states versus time for three different decay rates: $\Gamma_1 = 10000$, 1000, and 100 Hz. The renormalized Rabi frequencies for a sequence of laser pulses are taken as those used in Ref. [26]: $\Omega_1 = \Omega_4 = 2.0 \times 10^7$ Hz and $\Omega_2 = \Omega_3 = 1.7 \times 10^7$ Hz. Other laser parameters are chosen as follows: $\tau_1 = 3.0 \times 10^{-5}$ s, $\tau_4 = 1.8 \times 10^{-5}$ s, $\tau_d = 2.3 \times 10^{-5}$ s, and $T_1 = T_4 = 1.2 \times 10^{-5}$ s. Before the laser pulses ε_1 and ε_4 are turned on, the population of the $|g_1\rangle$ state linearly decreases with time due to the influence of Γ_1. At $t = 30$ μs, the actions of ε_1 and ε_4 are

over, and the population of the $|g_1\rangle$ state is transferred to the ground state $|g_3\rangle$. At $t = 50$ μs, under the action of the image pulses ε_1' and ε_4', the population of $|g_1\rangle$ is partly recovered. For $\Gamma_1 = 10$ kHz, finally only about 11% population is transferred to the $|g_1\rangle$ state. This indicates that the decay of $|g_1\rangle$ cannot be restrained by the STIRAP technique. However, in recent experiment, a new technique called "Mott-insulator" state was used to reduce the decay rate of the Feshbach state.[26] In the following calculation, we set $\Gamma_1 = 0$ for simplicity.

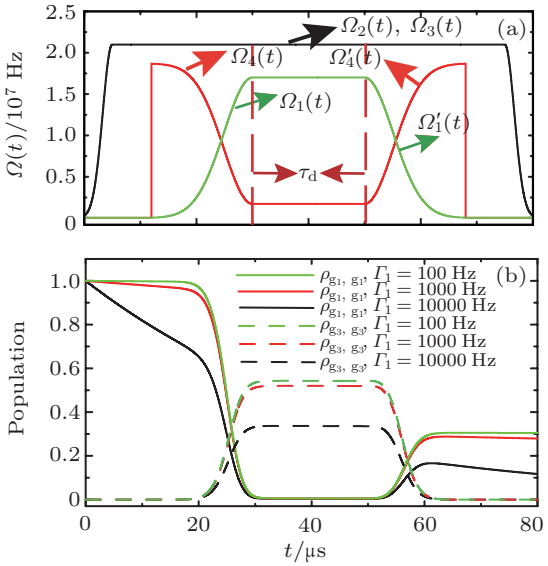


Fig. 2. (color online) (a) frequencies with the peak values $\Omega_1 = \Omega_4 = 2.0 \times 10^7$ Hz and $\Omega_2 = \Omega_3 = 1.7 \times 10^7$ Hz. (b) Populations of the $|g_1\rangle$ and $|g_3\rangle$ states for the decay rates of the Feshbach state: $\Gamma_1 = 10000$, 1000, and 100 Hz.

The evolution of population of the $|g_3\rangle$ state with time is illustrated in Fig. 3. We define the producing efficiency as $\eta_1 = \rho_{g_3,g_3}(t = 30\ \mu s)/\rho_{g_1,g_1}(t = 0)$, and the detecting efficiency as $\eta_2 = \rho_{g_1,g_1}(t = 80\ \mu s)/\rho_{g_1,g_1}(t = 0)$. At $t = 80$ μs, 31% of population returns to the $|g_1\rangle$ state. The producing efficiency is about 55% and the detecting efficiency is about 31%. These results are compatible with experimental data.[26]

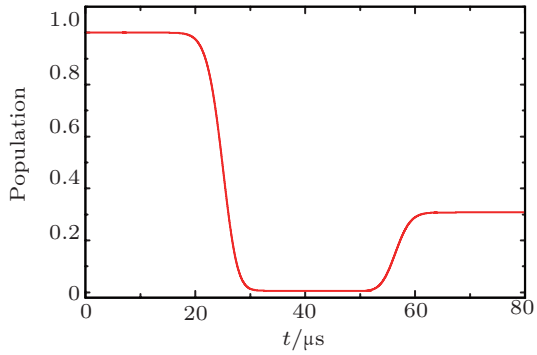


Fig. 3. (color online) Population of ground state $|g_1\rangle$ as a function of time for $\Delta_1 = \Delta_2 = 0$.

We now discuss the effect of detuning on the producing and detecting efficiencies. Figure 4(a) shows the producing efficiency η_1 versus the one-photon detunings Δ_1 and Δ_2. The detecting efficiency η_2 varying with Δ_1 and Δ_2 is shown in Fig. 4(b). When $\Delta_1 = \Delta_2 = 0$ (one-photon resonance), the producing efficiency η_1 reaches its peak value 55%. When Δ_1 and Δ_2 increase from -5.0×10^8 to 5.0×10^8 Hz, η_1 increases from 4% to 55% and then decreases to 1%. In the range of $\Delta_1 = \Delta_2$ from -1.5×10^8 Hz to 1.5×10^8 Hz, η_1 decreases slowly from 55% to 50%. The detecting efficiency η_2 displays a similar variation trend to the producing efficiency η_1. When $\Delta_1 = \Delta_2 = 0$, η_2 reaches its peak value 32%. When Δ_1 and Δ_2 increase from 0 to 1.0×10^8 Hz, η_2 decreases from 31% to 6%. In addition, when the negative detunings are used, the varying trends of η_1 and η_2 are roughly similar to those when the detunings are positive.

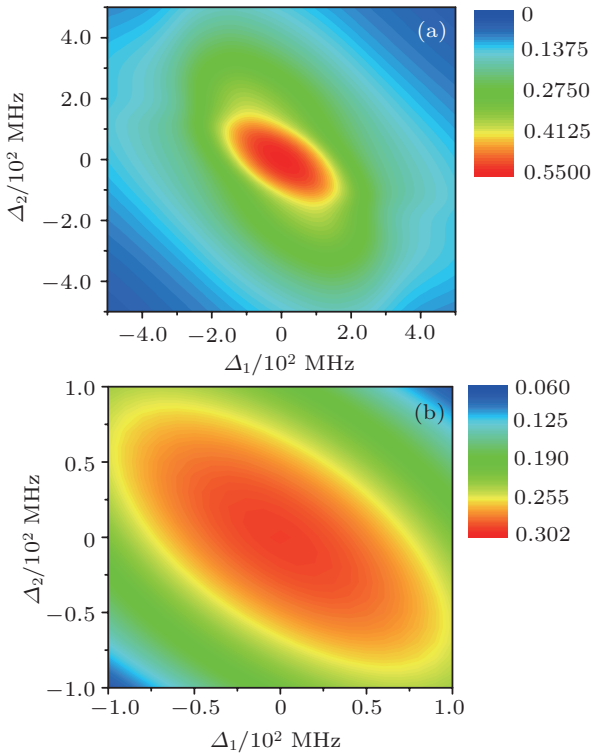


Fig. 4. (color online) (a) Producing efficiency versus detunings Δ_1 and Δ_2. (b) Detecting efficiency versus Δ_1 and Δ_2.

Figure 5 depicts the producing efficiency η_1 versus Ω_1, Ω_2, Ω_3, and Ω_4. Figure 6 shows detecting efficiency η_2 versus Ω_1, Ω_2, Ω_3, and Ω_4. Other parameters are the same as those in Fig. 3(a). When $\Omega_1 = 0$, the adiabatic passage is shut off, and almost all population remains on the $|g_1\rangle$ state. The η_1 and η_2 reach their respective peak value when $\Omega_1 = 5.0 \times 10^7$ Hz and then remains essentially unchanged when $\Omega_1 > 5.0 \times 10^7$ Hz. The η_1 and η_2 display a similar changing trend to Ω_2. With the increase in Ω_2 from 0 to 2.0×10^7 Hz, η_1 reaches its peak value 55% and η_2 reaches its peak values 31%. When Ω_2 increases to 8.0×10^7 Hz, η_1 decreases to 40% and η_2 decreases to 8%. The η_1 and η_2 reach their peak values at $\Omega_1 = 2.0 \times 10^7$ Hz and then decrease with the increase in Ω_3

from 2.0×10^7 to 8.0×10^7. The η_1 and η_2 display different changing tendency with the change of Ω_4. The η_1 increases to the peak value 69% and then decreases to 20% while η_2 increases to 82% and hereafter remains unchanged.

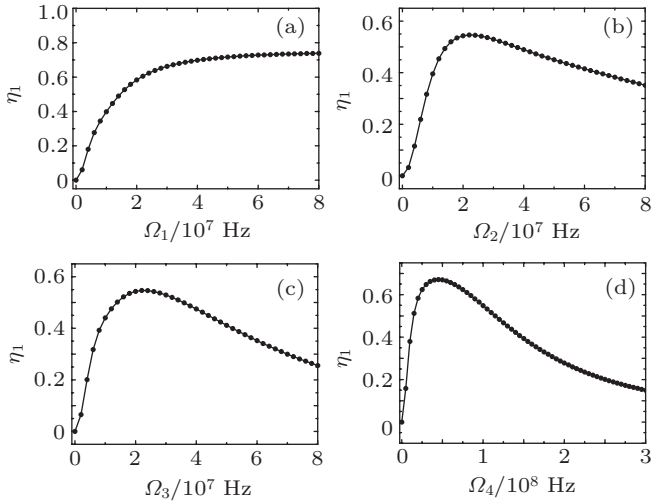


Fig. 5. Producing efficiency versus (a) Ω_1 with $\Omega_2=\Omega_3=1.7\times10^7$ Hz and $\Omega_4=2.0\times10^7$ Hz, (b) Ω_2 with $\Omega_1=\Omega_4=2.0\times10^7$ Hz and $\Omega_3=1.7\times10^7$ Hz, (c) Ω_3 with $\Omega_1=\Omega_4=2.0\times10^7$ Hz and $\Omega_2=1.7\times10^7$ Hz, (d) Ω_4 with $\Omega_2=\Omega_3=1.7\times10^7$ Hz and $\Omega_1=2.0\times10^7$ Hz. Other parameters are the same as those in Fig. 3(a).

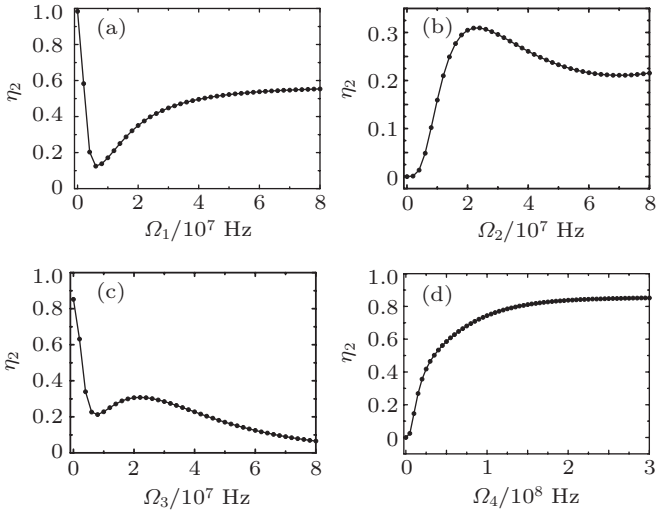


Fig. 6. Detecting efficiency versus (a) Ω_1 with $\Omega_2=\Omega_3=1.7\times10^7$ Hz and $\Omega_4=2.0\times10^7$ Hz, (b) Ω_2 with $\Omega_1=\Omega_4=2.0\times10^7$ Hz and $\Omega_3=1.7\times10^7$ Hz, (c) Ω_3 with $\Omega_1=\Omega_4=2.0\times10^7$ Hz and $\Omega_2=1.7\times10^7$ Hz, and (d) Ω_4 with $\Omega_2=\Omega_3=1.7\times10^7$ Hz and $\Omega_1=2.0\times10^7$ Hz. Other parameters are the same as those in Fig. 3.

4. Conclusion

We investigate theoretically how to produce and detect ultracold molecules via the multistate chainwise STIRAP by solving the quantum Liouville equation based on the multi-level Bloch model. The molecules formed in high vibrational states are transferred into lower vibrational state via two intermediate vibrational states. Numerical computation for the Cs_2 molecule shows that the producing efficiency reaches 55% and the detecting efficiency is 31%. Both the producing and detecting efficiencies depend strongly on the Rabi frequencies of four laser pulses. The decays of relevant states obviously reduce the producing and detecting efficiencies.

References

[1] Lambert J, Noel M W and Gallagher T F 2002 *Phys. Rev. A* **66** 053413
[2] Zhang W, Xie T, Huang Y, Wang G R and Cong S L 2013 *Chin. Phys. B* **22** 013301
[3] Wu J Z, Ma J, Ji Z H, Zhang Y C, Li Y Q, Wang L R, Zhao Y T, Xiao L T and Jia S T 2012 *Chin. Phys. B* **21** 093701
[4] Hua W, Li B and Liu X S 2011 *Chin. Phys. B* **20** 060308
[5] Hua W, Li B and Liu X S 2011 *Chin. Phys. B* **20** 010311
[6] Lin F, Zhang W, Zhao Z Y and Cong S L 2012 *Chin. Phys. B* **21** 073203
[7] Micheli A, Brennen G K and Zoller P 2006 *Nat. Phys.* **2** 341
[8] Chin C, Flambaum V V and Kozlov M G 2009 *New J. Phys.* **11** 055048
[9] Zelevinsky T, Kotochigova S and Ye J 2008 *Phys. Rev. Lett.* **100** 043201
[10] Koch C P, Luc-Koenig E and Masnou-Seeuws F 2006 *Phys. Rev. A* **73** 033408
[11] Koch C P, Kosloff R, Luc-Koenig E, Masnou-Seeuws F and Crubellier A 2006 *J. Phys. B* **39** S1017
[12] Zhang C Z, Zheng B, Wang J and Meng Q T 2013 *Chin. Phys. B* **22** 023401
[13] Aikawa K, Akamatsu D, Hayashi M, Oasa K, Kobayashi J, Naidon P, Kishimoto T, Ueda M and Inouye S 2010 *Phys. Rev. Lett.* **105** 203001
[14] Zhang Y C, Ma J, Wu J Z, Wang L R, Xiao L T and Jia S T 2013 *Phys. Rev. A* **87** 030503
[15] Wu J Z, Ji Z H, Zhang Y C, Wang L R, Zhao Y T, Ma J, Xiao L T and Jia S T 2011 *Opt. Lett.* **36** 2038
[16] Zhang Y C, Ma J, Li Y Q, Wu J Z, Zhang L J, Chen G, Wang L R, Zhao Y T, Xiao L T and Jia S T 2012 *Appl. Phys. Lett.* **101** 131114
[17] Chen D Y, Lu Z Z, Fan R W, Xia Y Q, Zhou Z G and Ji Y Q 2012 *Chin. Phys. B* **21** 083202
[18] Wang G R, Xie T, Zhang W, Huang Y and Cong S L 2012 *Phys. Rev. A* **85** 032706
[19] Chin C, Grimm R, Julienne P and Tiesinga E 2010 *Rev. Mod. Phys.* **82** 1225
[20] Mackie M, Fenty M, Savage D and Kesselman J 2008 *Phys. Rev. Lett.* **101** 040401
[21] Mackie M, Phou P, Boyce H, Shinn M and Katz L 2011 *Phys. Rev. A* **84** 043614
[22] Mackie M and Phou P 2010 *Phys. Rev. A* **82** 035602
[23] Bergmann K, Theuer H and Shore B W 1998 *Rev. Mod. Phys.* **70** 1003
[24] Winkler K, Lang F, Thalhammer G, Straten P V D, Grimm R and Denschlag J H 2007 *Phys. Rev. Lett.* **98** 043201
[25] Mark M J, Danzl J G, Haller E, Gustavsson M, Bouloufa N, Dulieu O, Salami H, Bergeman T, Ritsch H, Hart R and Nägerl H C 2009 *Appl. Phys. B* **95** 219
[26] Danzl J G, Mark M J, Haller E, Gustavsson M, Hart R, Aldegunde J, Hutson J M and Nägerl H C 2010 *Nat. Phys.* **6** 265
[27] Kuznetsova E, Pellegrini P, Côté R, Lukin M D and Yelin S F 2008 *Phys. Rev. A* **78** 021402